Hydrogenation of levulinic acid to gamma-valerolactone over anatase-supported Ru catalysts

Piskun, A. S.; Ftouni, J.; Tang, Z.; Weckhuysen, B. M.; Bruijnincx, P. C. A.; Heeres, H. J.

Published in:
Applied Catalysis A-General

DOI:
10.1016/j.apcata.2017.09.032

Publication date:
2018

Applied Catalysis A, General 549 (2018) 197–206

Contents lists available at ScienceDirect

Applied Catalysis A, General

journal homepage: www.elsevier.com/locate/apcata

Research Paper

Hydrogenation of levulinic acid to γ-valerolactone over anatase-supported Ru catalysts: Effect of catalyst synthesis protocols on activity

A.S. Piskun[a], J. Ftouni[b], Z. Tang[a], B.M. Weckhuysen[b], P.C.A. Bruijnincx[b], H.J. Heeres[a,*]

[a] Department of Chemical Engineering, ENTEG, University of Groningen, Nijenborgh 4, 9747 AG Groningen, The Netherlands
[b] Inorganic Chemistry and Catalysis, Debye Institute for Nanomaterials Science, Utrecht University, Universiteitsweg 99, 3584 CG Utrecht, The Netherlands

ARTICLE INFO

Keywords:
Biobased chemicals
Hydrogenation
Ru catalysts
Titania

ABSTRACT

γ-Valerolactone (GVL) is a value-added renewable chemical with great potential and can be obtained from biomass by the hydrogenation of levulinic acid (LA) using metal-based catalysts, such as Ru/TiO_2. We here report an in depth study of the effect of catalyst synthesis parameters on the performance of Ru/TiO_2 (anatase), varying the nature of the Ru-precursor and the conditions of the calcination and/or reduction step. Catalyst performance was evaluated under batch conditions at a hydrogen pressure of 45 bar and using either water (90 °C) or dioxane (150 °C) as solvent. The experiments showed that catalyst activity depends greatly on the Ru precursor used ($RuCl_3$, $RuNO(NO_3)_3$, $Ru(NH_3)_6Cl_3$). Best results when considering the turn-over frequencies (TOF) of the catalysts were obtained using the $RuNO(NO_3)_3$ precursor, whereas $RuCl_3$ performed better when considering the initial rate based on Ru intake. An intermediate calcination step and the use of a hydrogen-rich sweep gas during the final reduction step were shown to have a negative impact on catalyst activity. Characterization of the fresh catalysts by BET and TEM provided valuable insight in the relation between the catalyst structure and its activity.

1. Introduction

Levulinic acid (LA) is a major product of the controlled dehydration of the C6-sugars (D-glucose, D-mannose and D-galactose) in lignocellulosic biomass. It is recognized as an important carbohydrate-derived renewable platform molecule and has attracted considerable interest from a number of chemical companies [1,2]. The family of LA derivatives is large and some have much potential for commercialization. For instance, LA can be converted to 2-methyltetrahydrofuran (MTHF) and various levulinate esters, which may be used as gasoline and biodiesel additives, respectively [3–8]. δ-Aminolevulinic acid is a well-known herbicide and β-acetylacrylic acid has been proposed as a (co-)monomer for novel acrylate polymers [1]. Arguably, most attention has been devoted to the conversion of LA to γ-valerolactone (GVL), as GVL is considered as an important platform chemical in its own right and can be used as food additive, solvent and as precursor for fuel additives and bulk polymers [9–13]. The conventional way to produce GVL involves the hydrogenation of LA or its esters [14–16], with molecular hydrogen or an alternative hydrogen donor (e.g. formic acid), preferably using heterogeneous catalysts (Scheme 1). The intermediate 4-hydroxypentanoic acid (4-HPA) may be found in relatively high amounts when using water as the solvent, its exact amount depending on the relative rate of hydrogenation versus the rate of the intramolecular esterification reaction.

Recently, Liguori and Barbaro [17] published a comprehensive review on the direct catalytic conversion of renewable sources to GVL with an emphasis on the heterogeneous catalysts that have been used for this reaction. Noble metal-based catalysts are most commonly and successfully employed, with Ru-based ones in particular showing high activity and selectivity to GVL [14,18–21]. In addition to the nature of the active metal phase, the choice of support also has a large effect on catalyst performance, in particular on catalyst stability.

Activated carbons are the most widely used support for Ru in LA hydrogenation [22–24], mainly due to their good performance and availability [24–26], and as such Ru/C catalysts can be regarded as one of the benchmark catalysts for this reaction. Under continuous flow conditions and using water as the solvent, however, slow though irreversible deactivation of the Ru/C catalyst was observed, presumably due to Ru sintering and a reduction in specific surface area as a result of the deposition of carbonaceous deposits [15,22,25,27].

Various metal oxides, including SiO_2, Al_2O_3, Nb_2O_5, ZrO_2 and TiO_2, have been tested as a support for LA hydrogenation with Ru as the active metal [16,19,24,25]. A major advantage of such metal oxides over carbon supports is their mechanical and thermal stability, which

* Corresponding author.
E-mail address: h.j.heeres@rug.nl (H.J. Heeres).

http://dx.doi.org/10.1016/j.apcata.2017.09.032
Received 28 March 2017; Received in revised form 23 September 2017; Accepted 25 September 2017
Available online 28 September 2017

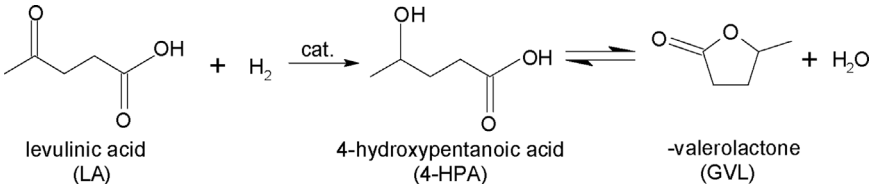

Scheme 1. Proposed reaction scheme for the catalytic hydrogenation of LA to GVL.

allows for repetitive regeneration and coke removal at elevated temperature. However, for some of these oxides, e.g. Al_2O_3 and SiO_2, the stability under hydrothermal, acidic conditions is known to be limited, which is of relevance for LA hydrogenations carried out in water or at high LA loadings [25,28]. Estimations of oxide support stability in pressurized water at 200 °C were recently provided by Lange using Pourbaix diagrams [2]. SiO_2 has the tendency to be converted into silica gel at all pH values, whereas Al_2O_3 is well-known to convert into boehmite (AlO(OH)) at pH values between 4.5 and 11.5. TiO_2, calculated to be stable over the entire pH range, and ZrO_2 are attractive alternatives [28], even though hydrated $Zr(OH)_4$ was found to be the thermodynamically most stable phase in water. Indeed, a screening study on LA hydrogenation involving 50 catalysts in a flow reactor system revealed that Pt on TiO_2 (P25 from Degussa) and ZrO_2 performed best, with constant GVL yields for runtimes exceeding 100 h (> 95 mol% at 200 °C and 40 bar H_2, 11 wt.% LA in GVL) [28]. LA hydrogenation studies in water as solvent comparing Ru/TiO_2 (P25) and Ru/ZrO_2 catalysts (both 1 wt.% Ru) in a batch set-up at 70 °C revealed that quantitative LA conversion could be achieved within 4 h with the Ru/TiO_2 catalysts, while Ru/ZrO_2 was less active and 92% LA conversion was observed after 6 h [29]. This enhanced hydrogenation activity of Ru/TiO_2 was attributed to a better Ru dispersion on TiO_2.

Recently, some of us reported on a catalyst screening study for LA hydrogenation in water (90 °C, 45 bar H_2) using a wide range of supported Ru-catalysts (1 wt.% Ru on C, CNT, Al_2O_3, TiO_2, ZrO_2, Nb_2O_5 and H-Beta-12.5) and again found that TiO_2 (anatase form, A100) performed better than for Ru/ZrO_2 in this solvent [30]. The results listed above thus show the potential of TiO_2 as support for this reaction and an overview of titania-supported Ru catalysts for LA hydrogenation is given in Table 1.

Some of these studies have shown that the phase composition of the TiO_2 support (anatase, rutile and combinations thereof) influences catalyst performance. For example, Al-Shaal et al. investigated the hydrogenation of LA using Ru supported on rutile and P25 TiO_2 (a 75:25 mixture of anatase-rutile) supports in ethanol and ethanol–water mixtures [25]. The rutile-supported catalyst gave no LA conversion in neither ethanol nor ethanol–water, whereas Ru/TiO_2 (P25) showed much better performance. Furthermore, a comparison of the catalytic transfer hydrogenation of levulinate esters using $Ru(OH)_x/TiO_2$ [31], with anatase, rutile and anatase-rutile titanias, showed the anatase-rutile-based catalyst to perform best (86% for TiO_2(A); > 99% for TiO_2(R) and TiO_2(A75:R25)). Recently, Ruppert et al. reported a detailed study on the influence of various TiO_2 supports (anatase, rutile and mixtures thereof) on the Ru-catalyzed LA hydrogenation [32]. A

Table 1
Literature overview on LA hydrogenation using Ru/TiO_2 catalysts in batch and continuous flow set-ups.

Catalyst	TiO_2 support	Ruthenium precursor	Solvent	T (°C)	H_2 pressure (bar)	Reaction time (h)	LA conversion (%)	GVL Selectivity (%)	Ref.
	Batch								
$Ru_{1\%}/TiO_2$	P25 (A75:R25)[a]	$RuNO(NO_3)_3$	dioxane	200	40	4	100	92	[19]
$Ru_{1\%}/TiO_2$	P25 (A75:R25)	$RuCl_3$	dioxane	200	40	0.6	100	99	[20]
$Ru_{5\%}/TiO_2$	Tronox (R100)	$Ru(acac)_3$	ethanol ethanol + H_2O	130	12	2.7	n.r.[d]- n.r.[d]-	– –	[25]
$Ru_{5\%}/TiO_2$	P25 (A75:R25)	$Ru(acac)_3$	ethanol ethanol + H_2O	130	12	2.7	68 81	92 88	[25]
$Ru_{2\%}/TiO_2$	P25 (A75:R25)	$RuCl_3$	H_2O	130	40	0.5	100	99	[29]
$Ru_{1\%}/TiO_2$	P25 (A75:R25)	$RuCl_3$	H_2O	130	40	3	95	99	
$Ru_{0.5\%}/TiO_2$	P25 (A75:R25)	$RuCl_3$	H_2O	70	40	4	100	99	
$Ru_{1\%}/TiO_2$	(A100)	$RuCl_3$	H_2O	90	45	5	93	85	[30]
$Ru(OH)_x/TiO_2$	ST−01[b] (A100)	$RuCl_3$	2-propanol	90	–	24	86	76	[31]
$Ru(OH)_x/TiO_2$	TTO−55[c](R100)	$RuCl_3$					> 99	49	
$Ru(OH)_x/TiO_2$	P25 (A75:R25)	$RuCl_3$					> 99	80	
$Ru_{1\%}/TiO_2$	P25 (A75:R25)	$Ru(acac)_3$	H_2O	30 70	50	1	64 99	62 95	[32]
$Ru_{1\%}/TiO_2$	P90 (A90:R10)	$Ru(acac)_3$	H_2O	30 70	50	1	60 100	60 100	[32]
$Ru_{1\%}/TiO_2$	(R100)	$Ru(acac)_3$	H_2O	30 70	50	1	40 95	40 83	[32]
$Ru_{1\%}/TiO_2$	ST-01 (A100)	$Ru(acac)_3$	H_2O	30 70	50	1	54 99	48 93	[32]
	Continuous flow								
$Ru_{0.4\%}/TiO_2$	P25 (A75:R25)	$RuCl_3$	H_2O	50	24	–	7	36	[33]
$Ru_{5\%}/TiO_2$	P25 (A75:R25)	$RuCl_3$	H_2O	270	n.r.[d]-	n.r.[d]-	52.6	44.3	[34]
$Ru_{1\%}/TiO_2$	P25 (A75:R25)	$RuCl_3$	H_2O	90	45	6	25	54	[35]

[a] A: Anatase, R: rutile.
[b] ST-01: anatase TiO_2, S_{BET} = 339 m^2/g (Ishihara Sangyo Co., Ltd.).
[c] TTO-55: rutile TiO_2, S_{BET} = 47 m^2/g (Ishihara Sangyo Co., Ltd.).
[d] Not reported.

Ru/TiO_2 (AR) catalyst (10–20% rutile) again proved to be more active than fully anatase-based ones. The lower activity of the latter was attributed to the presence of larger Ru particles and agglomerates on the surface and relatively small Ru nanoclusters predominantly found in micropores, thought to be inactive in the hydrogenation reaction. Activity of the anatase-based Ru catalyst could be improved by implementation of either a calcination step of the anatase support before impregnation to reduce the micropore volume or by avoiding a high temperature reduction step during catalyst synthesis by using a mild chemical reduction step [32].

Besides variations in support phase composition, many different synthetic procedures for titania-supported Ru catalyst preparation have been reported varying in the choice of, e.g., metal precursor, impregnation method and activation procedure (Table 1), which all may affect catalyst performance. Wet impregnation is most commonly used method for the synthesis of these Ru/TiO_2 catalysts [19,20,25,29], using Ru precursors such as $RuCl_3$, $Ru(NO)(NO_3)_3$, $Ru(acac)_3$, $Ru(NH_3)_6Cl_3$ or $Ru_3(CO)_{12}$ [19,20,25,29–35]. Limited information is available on the effects of these synthesis parameters on LA hydrogenation activity for Ru/TiO_2 catalysts. For a series of $Ni/\gamma\text{-}Al_2O_3$ catalysts, the effect of catalyst preparation method on catalytic activity for LA hydrogenation to GVL has been investigated [36]. Four different Ni catalysts were prepared via wet impregnation, incipient wetness impregnation, precipitation and flame spray pyrolysis, leading to different textural and, as a result, catalytic properties with wet impregnation giving the best results. Another example concerns the hydrogenation of LA to pentanoic acid using Ru supported on H-ZSM-5 [37], for which the use of $Ru(NH_3)_6Cl_3$ as precursor resulted in much better yields than when using $RuCl_3$.

To the best of our knowledge, a systematic study on the influence of several important synthesis variables (Ru precursor, calcination and/or reduction step) in the catalyst preparation procedure for the hydrogenation of LA with supported Ru catalysts has not been reported to date. We here report such an approach using Ru supported on pure anatase TiO_2. The support choice was fixed to reduce the complexity of possible variations during the catalyst synthesis procedure. In addition, we have recently shown good catalytic results for Ru on anatase TiO_2 [30]. Perusal of the literature on Ru/TiO_2 catalyzed LA hydrogenation (Table 1) finally shows that catalyst performance not only depends on support choice and catalyst synthesis parameters, but that a strong dependence on the choice of solvent can also be expected. Therefore, catalyst activity and selectivity to GVL were determined in both water and dioxane, the latter being a typical example of an organic solvent. It is well known that higher activities are attainable for reactions run in water compared to dioxane at otherwise similar conditions. As such, an optimum catalyst preparation procedure for catalysis in water not necessarily be the best for dioxane. Catalyst characterization (N_2 physisorption, Transmission Electron Microscopy (TEM) and Scanning Electron Microscopy (SEM) were carried out to rationalize the results and provided insight into the relation between catalyst performance and catalyst structure.

2. Experimental section

2.1. Materials

Levulinic acid (purity > 98%, less than 1 wt.% H_2O) and dioxane (purity > 99%) were purchased from Acros Organics, deuterium oxide (purity 99.9%) was purchased from Sigma-Aldrich. Hydrogen and nitrogen gas were from Linde Gas (purity > 99.9%). The ruthenium precursors, $RuCl_3{\cdot}xH_2O$ (35–40 wt.% Ru) and $Ru(NH_3)_6Cl_3$ (98 wt.% Ru) were supplied by Sigma-Aldrich; $RuNO(NO_3)_3$ (in dilute nitric acid, 1.5 wt.% Ru) was supplied by Acros Organics. All chemicals were used as received. TiO_2 support (≥99%, powder, average diameter of 156 nm (see Fig. S1, Supplementary information)) was obtained from Sigma-Aldrich and dried at 120 °C for 4 h in air before use. XRD analysis only shows peaks of the anatase formand clear peaks of the rutile phase are absent (Fig. S2, Supplementary information).

2.2. Analytical equipment

2.2.1. X-Ray diffraction (XRD)

The crystal form of the TiO_2 support was determined using X-ray diffraction (D8 Advance, Bruker) with filtered Cu K_α radiation and a wavelength of 1.5404 Å. The tube voltage was 40 kV, and the current was 30 mA. The 2θ scanning rate was 0.02°/min in a range from 5 to 80°.

2.2.2. Transmission electronic microscopy (TEM)

TEM measurements in bright field mode were conducted with a CM12 microscope (Philips), operating at 120 keV. Samples were made by ultra-sonication in ethanol and dropping the suspension onto carbon coated 400 mesh copper grids. Images were taken on a slow scanning CCD camera. The metal particle size distribution is calculated by measuring at least 100 particles with the software Nano Measurer 1.2.

2.2.3. Scanning electronic microscopy (SEM)

The average size of the TiO_2 particles was determined using Scanning Electron Microscope Jeol JSM-7000F (Field Emission Scanning Electron Microscope). For this purpose, the size of about 300 particles was measured.

2.2.4. Nitrogen physisorption experiments

Nitrogen physisorption experiments were carried out in a Micromeritics ASAP 2020 at −196.2 °C. The samples were degassed in vacuum at 200 °C for 10 h. The surface area was calculated using the standard BET method (SBET). The single point gas adsorption pore volume (V_T) was calculated from the amount of gas adsorbed at a relative pressure of 0.98 in the desorption branch. The pore size distributions (PSD) were obtained from the BJH method using the adsorption branch of the isotherms. The mean pore size was taken as the position of the PSD maximum. The t-plot method was employed to quantify the micropore volume (V_M).

2.3. Catalyst preparation

A total of sixteen Ru/TiO_2 catalysts were synthesized via a standardized wet impregnation procedure. The anatase titania support was dried (120 °C for 4 h in air) before use. The ruthenium loading was kept constant at 1 wt.% Ru for all catalysts. A number of parameters were varied: Ru precursor ($RuCl_3{\cdot}xH_2O$; $RuNO(NO_3)_3$ or $Ru(NH_3)_6Cl_3$), calcination step (with or without) and the amount of hydrogen in the gas phase during the reduction step (5, 10, 50 or 100 vol.% H_2). Throughout this paper, the catalysts are abbreviated based on the precursor used for its preparation and the calcination/reduction procedure. For instance, Ru/TiO_2(Cl,N,10) is a catalyst made using $RuCl_3$ as the precursor, without calcination and reduced in an atmosphere with 10 vol.% H_2 in nitrogen.

A typical catalyst synthesis entailed the dissolution of a required amount of the precursor in 25 mL of water while stirring (1100 rpm) for 30 min at 30 °C to obtain a homogeneous solution. The titania support (1 g) was added gradually to the precursor solution under stirring. Subsequently, the temperature was increased to 85 °C and kept until complete evaporation of the water (after about 19 h). After the impregnation, the catalyst was calcined and/or reduced. Catalysts prepared without a calcination step were directly reduced after the impregnation. When the catalysts were calcined, this was done after impregnation, followed by the reduction step. Calcination was performed using a Micrometrics AutoChem II 2920 system at 450 °C (heating rate 2 °C/min) in a nitrogen atmosphere (N_2 flow of 100 mL/min) for 4 h. The reduction step was carried out in the same system at 400 °C for 4 h. Either a N_2/H_2 mixture (with variable composition) or

pure H_2 was used, the total gas flow rate was maintained at a flow rate of 100 mL/min.

2.4. Catalytic hydrogenation of LA

LA hydrogenation reactions were performed according to previously published standard conditions for water [38], and dioxane [39]. The hydrogenation reactions using water as the solvent were performed in a stainless steel batch autoclave (100 mL, Parr Instrument Company). The heating mantel of the autoclave was equipped with electric heating rods and a cooling coil (using water) for proper temperature control. The reactor content was agitated using an overhead stirrer (Heidolph, RZR 2102 control). The temperature (90 °C) and hydrogen pressure (45 bar) were measured online with a Eurotherm 2208e. For liquid sampling during the reactions, the reactor was equipped with a dip-tube. LA (2.9 g) was dissolved in water (40 mL, 0.6 M) and catalyst (0.06 g, LA/Ru molar ratio of 4350) were introduced in the autoclave. The stirrer was started (2000 rpm) and the system was flushed with nitrogen for 5 min. The mixture was heated to the desired temperature and subsequently hydrogen was admitted to the reactor to 45 bar. This moment is set as t = 0 min. During the reaction, hydrogen was regularly admitted to the reactor to keep the pressure constant at 45 bar. The information has been added in the experimental section in the manuscript. 16 catalysts were prepared and tested for the hydrogenation reaction in water and dioxane. The hydrogenation result for one of the catalysts (Ru/TiO2(NO,N,100, particle size 4.7 nm) in water was discarded from the dataset as hardly any reactivity was observed, likely due to an unknown experimental error.

The reactions in dioxane were performed in a 50 mL Parr batch autoclave at a temperature of 150 °C for 4 h using a hydrogen pressure of 45 bar and a stirring speed of 1250 rpm. The tests were typically performed using 27.8 g of dioxane, 7.37 wt.% of levulinic acid (2.2 g, 0.63 M) with 0.06 g of catalyst (LA/Ru molar ratio of 3200). Then the autoclave was purged three times with argon after which the reaction mixture was heated to reaction temperature and charged with H_2. This was taken as the starting point of the reaction; during the reaction samples were taken regularly, filtered and 1 wt.% of anisole was added as internal standard to the samples. At the end of the reaction, the autoclave was cooled rapidly to room temperature in an ice bath, after which the remaining H_2 was released.

An overview of reaction conditions is given in Table 2.

2.5. Determination of the concentrations of LA, GVL and 4-HPA in the liquid phase

2.5.1. Analyses of the reaction products from LA hydrogenation in water

The composition of the aqueous reaction mixtures (LA, 4-HPA and GVL) was determined quantitatively by ^{1}H NMR. NMR analysis proved to be the most reliable method for the quantification of 4-HPA, which is difficult to determine by GC or HPLC [35]. A sample (approximately 200 μL) was weighed, dissolved in D_2O and dioxane (internal standard, 10 μL) was added. All spectra were integrated using MestReNova software. The number of moles of a component in the sample was calculated using Eq. (1):

$$mol_a = mol_s \times \left(\frac{Integral(analyte)}{Integral(int.\ stand.)} \right) \times \frac{N_s}{N_a} \quad (1)$$

where N_a is the number of hydrogen atoms of the NMR resonances used for the calculation (δ 2.1 ppm for LA (3 hydrogen atoms), δ 1.03 ppm for 4-HPA (3 hydrogen atoms), δ 1.3 ppm for GVL (3 hydrogen atoms)) and N_S is 8, being the number of hydrogen atoms of dioxane at δ 3.6 ppm. The concentrations of LA, GVL and 4-HPA in the samples were calculated using Eq. (2).

$$C_a = \frac{mol_a}{V_t} \times D_f \quad (2)$$

Where V_t is the volume of the mixture in NMR tube and D_f the dilution factor, which was calculated as follows (Eq. (3)):

$$D_f = \frac{mass\ of\ the\ sample\ in\ NMR\ tube + mass\ of\ D_2O + mass\ of\ internal\ standard}{mass\ of\ the\ sample\ in\ NMR\ tube} \quad (3)$$

2.5.2. Analyses of the reaction products from LA hydrogenation in dioxane

Reaction products were analyzed using a Shimadzu GC-2010A gas chromatograph equipped with a CPWAX 57-CB column (25 m × 0.2 mm × 0.2 μm) and FID detector, using authentic samples for calibration.

2.6. Definitions

The conversion of LA and the yield and selectivity for the products (4-HPA and GVL) were calculated according to Eq. (4)–(6).

$$X_{LA} = \frac{C_{LA,0} - C_{LA}}{C_{LA,0}} \times 100\% \quad (4)$$

$$Y_{GVL} = \frac{C_{GVL}}{C_{LA,0}} \times 100\%,\ Y_{4-HPA} = \frac{C_{4-HPA}}{C_{LA,0}} \times 100\% \quad (5)$$

$$S_i = \frac{Y_i}{X_{LA}} \times 100\% \quad (6)$$

Where X_{LA} is the conversion of LA (mol.%); $C_{LA,0}$ the initial concentration of LA (mol/L); C_{LA} the concentration of LA at a certain time t (mol/L); Y_{GVL} the yield of GVL (mol.%); $Y_{4\text{-HPA}}$ the yield of 4-HPA (mol.%) and S_i the selectivity to GVL or 4-HPA (mol.%).

The initial reaction rate (R_0, mol/mol$_{Ru}$ s) was determined from the experimentally obtained concentration-time profiles using a procedure given by Fogler [40]. For this purpose, the concentration time profile was modeled using a higher order polynome. The initial rate was determined by differentiation of the polynome and setting the value for the time at zero.

The turnover frequency (TOF, s^{-1}) was calculated according to Eq. (7).

$$TOF = \frac{R_0}{D_{Ru}} \quad (7)$$

Where R_0 is the initial reaction rate (mol/mol$_{Ru}$ s) and D_{Ru} is the dispersion of ruthenium, which was calculated as follows (Eq. (8)):

$$D_{Ru} = \frac{6 \times V_{Ru}}{a_{Ru} \times d_{Ru}} \quad (8)$$

where V_{Ru} is the volume occupied by a bulk Ru atom (0.01365 nm^3), a_{Ru} is an area per Ru atom (0.0635 nm^2) and d_{Ru} is the average diameter of a Ru particle (nm, taken from the TEM data).

Table 2
Standard reactions conditions for LA hydrogenation with the Ru/TiO_2 catalysts in batch.

Solvent	water [38]	dioxane [39]
LA initial concentration (mol/L)	0.63	0.64
Solvent intake (mL)	40	28
Temperature (°C)	90	150
Hydrogen pressure (bar)	45	45
Catalyst intake (g)	0.060	0.060
LA/Ru molar ratio	4350	3200
Stirring rate (rpm)	2000	1250
Reaction time (h)	4	4

Table 3
Catalyst characterization data for the different Ru/TiO_2 catalysts, including catalyst labeling scheme.

#		Ru precursor	Hydrogen (vol.%) in reduction gas[a]	Calcination[b]	BET Surface area (m^2/g)	Micropore volume (cm^3/g)	d_{Ru} (nm) (TEM)
1	Ru/TiO_2(Cl,N,10)	$RuCl_3$	10	No	13	2.4×10^{-4}	2.2 ± 0.7
2	Ru/TiO_2(Cl,N,50)	$RuCl_3$	50	No	12	4.4×10^{-4}	2.1 ± 0.7
3	Ru/TiO_2(Cl,N,100)	$RuCl_3$	100	No	10	≈0	8.4 ± 4.5
4	Ru/TiO_2(Cl,Y,100)	$RuCl_3$	100	Yes	12	≈0	14.2 ± 6.6
5	Ru/TiO_2(Cl,Y,50)	$RuCl_3$	50	Yes	n.d.[c]	n.d.	10.1 ± 4.6
6	Ru/TiO_2(Cl,Y,10)	$RuCl_3$	10	Yes	n.d.	n.d.	5.9 ± 2.9
7	Ru/TiO_2(Cl,Y,5)	$RuCl_3$	5	Yes	n.d.	n.d.	5.2 ± 3.7
8	Ru/TiO_2(Cl,Y,0)	$RuCl_3$	No	Yes	n.d.	n.d.	4.1 ± 1.8
9	Ru/TiO_2(NO,N,10)	$RuNO(NO_3)_3$	10	No	12	3.9×10^{-4}	4.7 ± 2.1
10	Ru/TiO_2(NO,N,50)	$RuNO(NO_3)_3$	50	No	11	2.1×10^{-4}	1.1 ± 0.1
11	Ru/TiO_2(NO,Y,100)	$RuNO(NO_3)_3$	100	Yes	13	≈0	7.7 ± 7.0
12	Ru/TiO_2(NH_3,N,10)	$Ru(NH_3)_6Cl_3$	10	No	12	3.7×10^{-4}	1.5 ± 0.5
13	Ru/TiO_2(NH_3,N,50)	$Ru(NH_3)_6Cl_3$	50	No	9	≈0	3.1 ± 0.8
14	Ru/TiO_2(NH_3,N,100)	$Ru(NH_3)_6Cl_3$	100	No	13	≈0	4.2 ± 1.1
15	Ru/TiO_2(NH_3,Y,100)	$Ru(NH_3)_6Cl_3$	100	Yes	13	≈0	1.4 ± 0.6

[a] Reductions always performed at 400 °C, make up gas is nitrogen.
[b] Calcination performed at 450 °C under nitrogen atmosphere.
[c] n.d.: not determined.

3. Results and discussion

3.1. Catalyst characterization

Sixteen Ru/TiO_2 catalysts were synthesized using $RuCl_3 \cdot xH_2O$, $RuNO(NO_3)_3$, $Ru(NH_3)_6Cl_3$ as Ru precursors, in/excluding a calcination step, and with different hydrogen partial pressures during the reduction step (5, 10, 50 or 100 vol.% H_2). Relevant properties of the various Ru/TiO_2 catalysts were determined (BET surface area, micropore volume and the average Ru nanoparticle size) and the results are provided in Table 3. N_2-physisorption analysis of fresh catalysts show that the surface areas are between 13 and 9 m^2/g, which are lower than for the bare anatase TiO_2 support (17 m^2/g). The average Ru particle size was determined with TEM (Table 3) and two representative TEM pictures are shown in Fig. 1. The average Ru nanoparticle size varied considerably over the series, ranging from 1.1 to 14.2 nm. In some cases, especially when the Ru nanoparticle sizes are larger than 6 nm, considerable particle agglomeration was observed.

The observation on the basis of TEM that well-dispersed Ru on TiO_2 (A100) with small average Ru nanoparticle sizes are attainable for some of the catalysts is surprising considering a recent study on Ru/TiO_2 (A100) [32]. Here, the wet impregnation of ruthenium ($Ru(acac)_3$ on large surface-area TiO_2 (A100, 83–336 m^2/g), followed by calcination at 200 °C in air and a reduction at similar conditions with hydrogen resulted in an inhomogeneous metal distribution with very large Ru nanoparticles (as seen by TEM) and small ones in the micropores. A Ru/TiO_2 (A100) catalyst for which the support was calcined at high temperature before impregnation to reduce microporosity showed no particle agglomerates and a rather homogeneous distribution was obtained with an average Ru particle size of 4.5 nm. Comparison between our results and these given above is difficult as the anatase support used in our study has a far lower BET surface area (17 m^2/g versus 83–336 m^2/g in [32]). However, it shows that the catalyst preparation procedure is of high importance and under optimum conditions, highly dispersed Ru/TiO_2 (A100) can be obtained.

3.2. Hydrogenation experiments using the anatase-supported Ru catalysts

Initial hydrogenation experiments were performed with Ru/TiO_2(Cl,N,10) in both water and dioxane. Standard reaction conditions were selected based our previous results [19,38,39], and are given in Table 2. The lower reaction temperature selected for the reaction in water (90 °C) compared to dioxane (150 °C) reflects the surprisingly high activity of Ru-based hydrogenation catalysts under aqueous conditions, for which the underlying reasons have been recently discussed [15,17,19,38,41,42]. The hydrogen pressure was set at 45 bar for all experiments. Concentration-time profiles for the main components (LA, 4-HPA and GVL) under these standard reaction conditions are shown in Fig. 2.

In the case of water as the reaction medium, substantial amounts of 4-HPA are formed, in line with our own observations and literature data

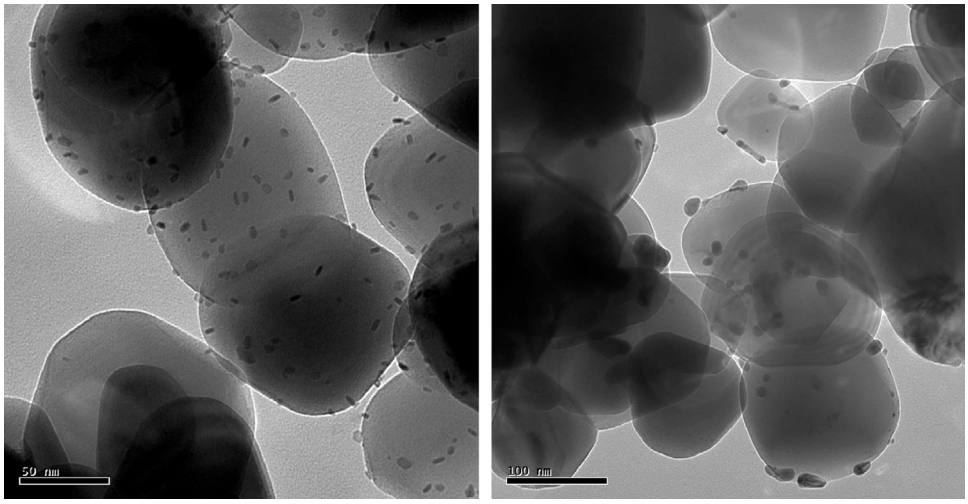

Fig. 1. TEM image of Ru/TiO_2(Cl,Y,0) (left) and Ru/TiO_2(Cl,Y,50) (right).

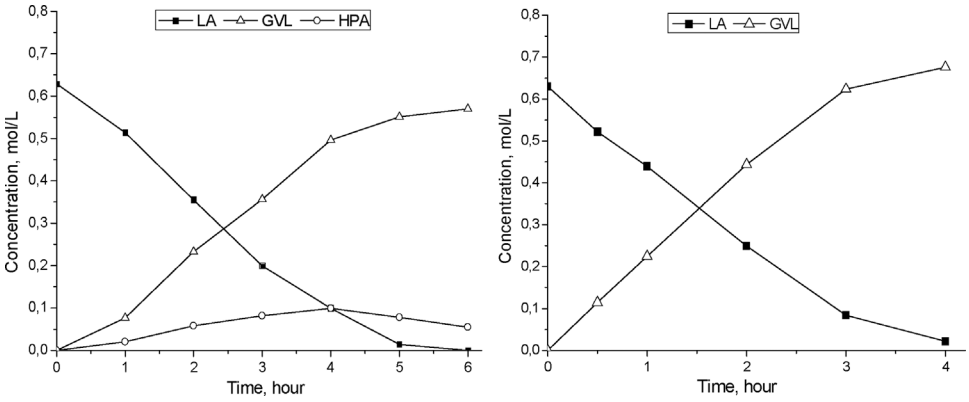

Fig. 2. Concentration-time reaction profiles for the hydrogenation of LA using $Ru/TiO_2(Cl,N,10)$ catalyst (#1) in water (left) and dioxane (right) under standard reaction conditions (Table 2).

[23,38,41]. Other intermediates (e.g. α-angelicalactone) or consecutive hydrogenation products of GVL (e.g., 1,4-pentanediol or 2-methyltetrahydrofuran) were not detected. Full conversion of LA was achieved within 6 h with 89% selectivity to GVL, the remainder being 4-HPA (Fig. 2). The intramolecular esterification of 4-HPA is known to be an equilibrium reaction with an equilibrium constant of about 16 [38]. The ratio of GVL/4-HPA obtained here after 6 h of reaction is 5, indicating that the two components are not yet at equilibrium.

The reaction in dioxane at 150 °C gave almost quantitative LA conversion after 4 h (Fig. 2), with full selectivity to GVL. No 4-HPA was detected in dioxane, as the intramolecular esterification reaction to GVL is much faster in organic solvents than in water due to equilibrium considerations (Scheme 1) [38].

3.3. Effect of variation of the Ru-precursor on catalytic activity

Variation of the Ru precursor at otherwise fixed synthesis conditions (i.e., no calcination and direct reduction with 10 vol.% H_2) gave the catalysts $Ru/TiO_2(Cl,N,10)$, $Ru/TiO_2(NO,N,10)$ and $Ru/TiO_2(NH_3,N,10)$ for which LA hydrogenation activity is shown in Fig. 3 and a compilation of the data is given in Table 4.

Remarkable differences in catalyst activity were observed for the three precursors, with the trends in activity being the same in both solvents.The catalyst prepared with $RuCl_3$ was the most active in both cases (Table 4), intermediate activity was found for $RuNO(NO_3)_3$ and lowest LA conversions was seen after 4 h for $Ru(NH_3)_6Cl_3$. In all cases, GVL was the major product, with, as expected, minor amounts of the intermediate 4-HPA for the reactions performed in water.

However, the general trend regarding LA conversion after 4 h is not exactly the one as described above for catalysts prepared by a direct reduction with 10 vol.% H_2. In general, the catalysts prepared with $RuCl_3$ and $RuNO(NO_3)_3$ gave the highest LA conversion after 4 h (Table 4). The highest activity for a catalyst prepared using the $RuCl_3$ precursor in water was observed for catalyst 1 (86% LA conversion), compared to 77% LA conversion when using the $RuNO(NO_3)_3$ precursor (catalyst 10). These highest conversions were obtained for the uncalcined catalysts which were reduced at relatively low hydrogen partial pressures. For catalysts made with the $Ru(NH_3)_6Cl_3$ precursor, LA conversions were in general by far lower than for the other two precursors and best performance was found for catalyst 12 (24% LA conversion). The choice of Ru precursors will influence the average Ru particle size, which is expected to play a large role in determining catalyst activity. In this study, the highest activity is observed for the Ru catalyst with an intermediate Ru particle size ($Ru/TiO_2(Cl,N,10)$, 2.2 nm). In addition, the Ru oxidation state might play a role as well, with Ru^0 nanoparticles assumed to be the catalytically active species [43], even though RuO_2 species may also play a role [41,44,45].

3.4. Effect of reduction procedure on catalyst activity

For a number of catalysts, prepared with $RuCl_3$ as the precursor, the partial pressure of hydrogen was varied in the reduction step (10, 50 and 100 vol.% H_2 in N_2/H_2 mixture, 1 bar). The results obtained with the catalysts ($Ru/TiO_2(Cl,N,10)$, $Ru/TiO_2(Cl,N,50)$ and $Ru/TiO_2(Cl,N,100)$ in Table 4) under standard conditions in both solvents are presented in Fig. 4.

The partial pressure of hydrogen during the catalyst reduction step has a profound influence on activity. Again the order of activity is the same for both solvents, with the best results obtained with the catalyst reduced at 10 vol.% of H_2. The TEM results show the same particle sizes of around 2.2 nm for the reduction with 10 and 50 vol.% H_2, while 100 vol.% H_2 leads to agglomeration and an average particle size of 8.4 nm. The catalytic results obtained with $Ru/TiO_2(Cl,N,10)$ and $Ru/TiO_2(Cl,N,50)$ differ considerably, despite the same TEM Ru particle size and indicate that factors other than mere particle size affect catalytic activity (*vide infra*).

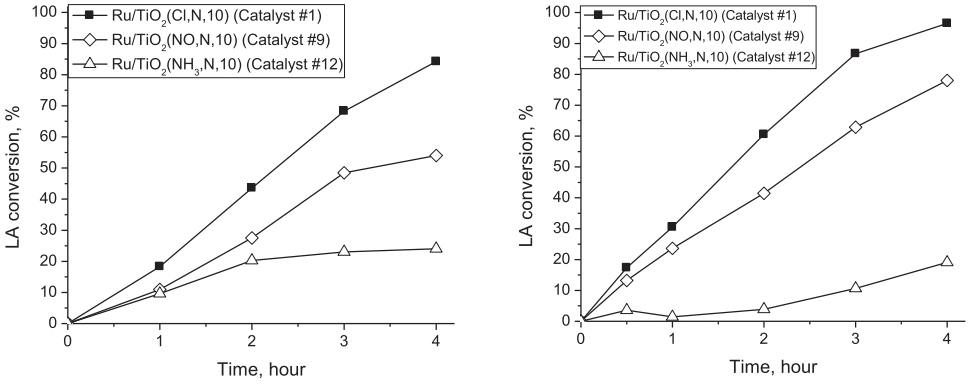

Fig. 3. LA conversion versus time using Ru/TiO_2 catalysts from three different precursors in water (left) and in dioxane (right) under standard reaction conditions (Table 2).

Table 4
Overview of results for the hydrogenation of LA using various Ru on titania catalysts in water and dioxane.

#	Catalyst name	Solvent	LA conv. (mol.%)[a]	Initial reaction rate (mol/mol$_{Ru}$ s)	Selectivity GVL (mol.%)[a]	Selectivity 4-HPA (mol.%)[a]	Yield GVL (mol.%)[a]
1	Ru/TiO_2(Cl,N,10)	H_2O	86	3.20×10^{-1}	92	7	79
		Dioxane	96	2.12×10^{-1}	100	–	96
2	Ru/TiO_2(Cl,N,50)	H_2O	69	2.63×10^{-1}	93	7	64
		Dioxane	69	1.94×10^{-1}	97	–	67
3	Ru/TiO_2(Cl,N,100)	H_2O	5	4.57×10^{-2}	83	17	4
		Dioxane	7	5.31×10^{-1}	100	–	7
4	Ru/TiO_2(Cl,Y,100)	H_2O	1	1.14×10^{-2}	99	1	1
		Dioxane	4	2.30×10^{-1}	100	–	5
5	Ru/TiO_2(Cl,Y,50)	H_2O	15	9.14×10^{-2}	87	12	13
6	Ru/TiO_2(Cl,Y,10)	H_2O	16	6.85×10^{-2}	70	29	11
7	Ru/TiO_2(Cl,Y,5)	H_2O	15	2.28×10^{-2}	91	9	14
8	Ru/TiO_2(Cl,Y,0)	H_2O	9	4.57×10^{-2}	41	59	4
9	Ru/TiO_2(NO,N,10)	H_2O	55	2.97×10^{-1}	91	8	50
		Dioxane	78	2.48×10^{-1}	92	–	71
10	Ru/TiO_2(NO,N,50)	H_2O	77	2.29×10^{-1}	94	6	72
		Dioxane	89	2.83×10^{-1}	92	–	82
11	Ru/TiO_2(NO,Y,100)	H_2O	18	1.14×10^{-1}	87	13	16
		Dioxane	2	3.18×10^{-1}	100	–	29
12	Ru/TiO_2(NH_3,N,10)	H_2O	24	1.94×10^{-1}	50	48	12
		Dioxane	19	7.08×10^{-2}	80	–	16
13	Ru/TiO_2(NH_3,N,50)	H_2O	3	1.14×10^{-3}	76	23	2
		Dioxane	7	5.31×10^{-3}	86	–	6
14	Ru/TiO_2(NH_3,N,100)	H_2O	5	1.37×10^{-2}	90	9	5
		Dioxane	10	4.6×10^{-2}	50	–	5
15	Ru/TiO_2(NH_3,Y,100)	H_2O	19	5.71×10^{-2}	87	13	16
		Dioxane	27	4.07×10^{-1}	78	–	21

[a] After 4 h batch time.

3.5. Effect of an intermediate calcination step on catalyst activity

The effect of a calcination step for Ru-catalyzed reactions has been reported in a number of studies. For instance, Luo et al. reported a negative effect on activity for the hydrogenation of LA in dioxane using a Ru/H-ZSM-5 catalyst [37]. The formation of highly mobile RuO_x species during the calcination step and subsequent sintering, was mentioned as the most likely reason. Ruppert et al. showed that avoiding a thermal treatment step in the catalyst preparation protocol was beneficial for catalytic activity for LA hydrogenations using Ru/TiO_2 (A100) in water [32]. This finding was attributed to a lowering of the average Ru particle size for the mild chemical treatment compared to calcination, leading to higher catalyst activities. The negative effect of a high temperature calcination step on the average Ru particle diameter (and catalytic activity) was also observed for the hydrogenation of *o*-xylene over Ru/TiO_2, Ru/Al_2O_3 and Ru/SiO_2 catalysts [46], again rationalized by agglomeration of Ru particles as a consequence of the high migration rates of RuO_2 species at elevated temperature [47,48].

We tested the effect of an intermediate calcination step during catalyst preparation on the catalytic activity in water for the catalysts prepared with the $RuCl_3$ precursors and the results are given in Fig. 5.

An intermediate calcination step negatively affects catalyst performance, as clearly demonstrated by the lower activity seen for all calcined catalysts when using $RuCl_3$, in line with the literature data reported above. Calcination indeed led to an increase in average Ru nanoparticle size when using $RuCl_3$ as precursor for catalyst synthesis, see Fig. 6 for details. However, for catalyst prepared with the $Ru(NH_3)_6Cl_3$ precursor, the calcined sample (catalyst 15) has a lower average Ru nanoparticle size than the uncalcined one (catalyst 14). Whether this is specific for catalysts prepared with the $Ru(NH_3)_6Cl_3$ precursor cannot be concluded unequivocally as the dataset is too limited, with only two samples for Ru $(NH_3)_6Cl_3$ compared to seven for $RuCl_3$.

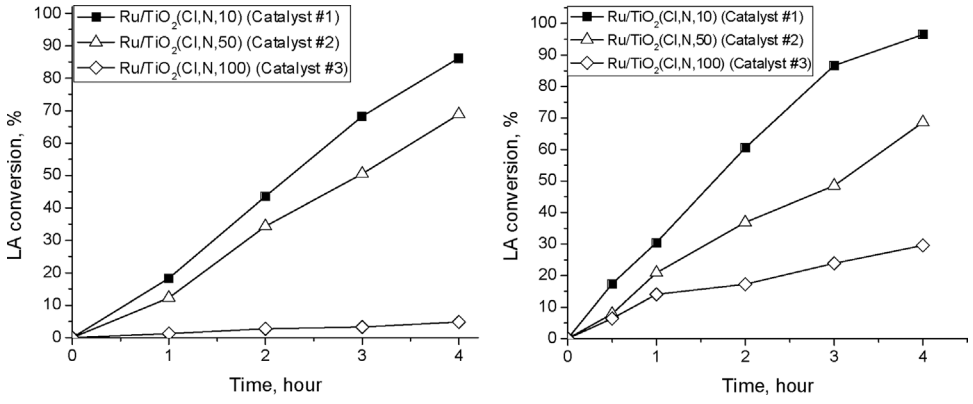

Fig. 4. Effect of hydrogen amount in the reduction gas during activation on LA conversion over Ru/TiO_2 (1 wt.% Ru) catalysts in water (left) and in dioxane (right) under standard reaction conditions (Table 2).

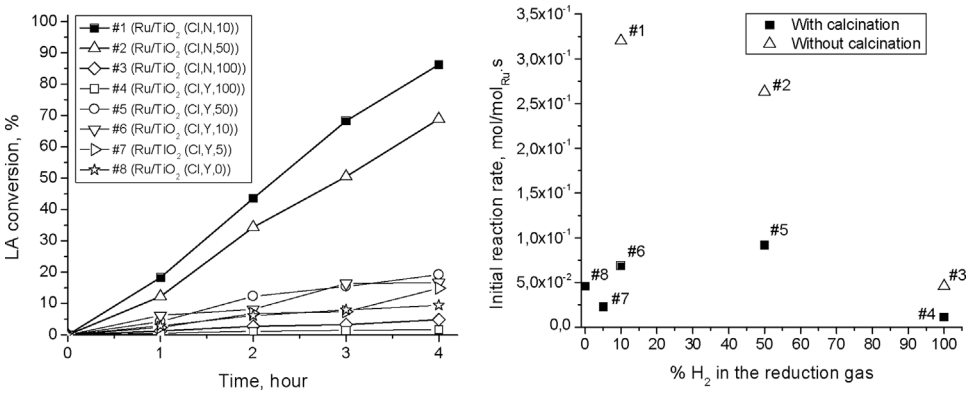

Fig. 5. Effect of the composition of the reduction gas and the use of an intermediate calcination step on the initial rate for the catalytic hydrogenation of LA in water for various Ru/TiO_2 catalysts (prepared using $RuCl_3$ as the precursor) under standard reactions conditions (Table 2).

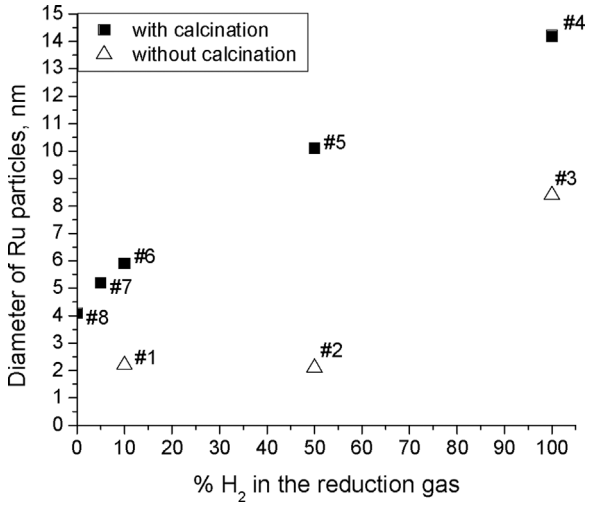

Fig. 6. Effect of the hydrogen amount in the reduction gas on the Ru particle size diameter for Ru/TiO_2 catalysts prepared with $RuCl_3$ precursor with and without a calcination step.

The effect of the partial pressure of hydrogen during the reduction step on catalyst activity of the calcined catalysts reveals the presence of an optimum value for intermediate hydrogen levels (Fig. 5). This might be the result of a balance in the average Ru particle diameter and extent of Ru reduction, which are expected to oppositely affect catalyst activity. TEM analysis (Fig. 6) shows that higher amounts of H_2 in the reduction step for the calcined samples led to sintering, which is expected to have a negative effect on catalytic activity.

3.6. Discussion

3.6.1. Effect of ruthenium particle size on catalytic activity for LA hydrogenation in water

The effect of the Ru nanoparticle size on catalytic activity for the hydrogenation of LA in water was investigated by comparing the initial rate of all reactions ($mol/mol_{Ru}.s$) and TOF (s^{-1}) versus the average Ru nanoparticle diameter as determined by TEM, see Fig. 7. The TOF values are a better activity performance indicator as these are normalized on the surface Ru atoms (based on TEM particle size data).

For catalysts, prepared with the $RuCl_3$ precursor, a volcano type plot is found for the initial rate as function of Ru particle size, with the highest activity for Ru nanoparticles with an average diameter of about 2 nm (Fig. 7, left). A similar trend can be seen for the catalysts prepared with the other precursors.

A number of papers have reported the effects of Ru nanoparticle size on catalytic activity for hydrogenation reactions with Ru on TiO_2 catalysts. Ruppert et al. [32], reported that the optimum Ru particle size for LA hydrogenation (in terms of LA conversion after a fixed batch time) for Ru/TiO_2 (A100) is in the range of 3–4 nm. The authors proposed that the activity for smaller Ru particles (< 1 nm) is lower as these are present in the micropores and thus less available for the hydrogenation reaction amongst others due to diffusion limitations [32]. Primo et al. examined the influence of metal nanoparticle size of Ru/TiO_2 (0.64 wt.% Ru) catalysts for the hydrogenation of lactic acid to 1,2-propanediol [49]. When increasing the Ru particle diameter from 2 to 10 nm by subjecting the catalysts to a calcination step at 400 °C, the product yield decreased from 99 to 38%.

TOF values, expressed as mol LA converted per mol of surface Ru per s, as a function of the Ru nanoparticle size (Fig. 7) show volcano type plots with a maximum TOF within the range. This implies that LA hydrogenation is structure sensitive for these catalysts. Surface sites of different configuration (e.g. ensembles of surface atoms), of which the concentration is a function of particle size and shape, then contribute differently to the observed, averaged reaction rate. Detailed overviews on structure sensitive (hydrogenation) reactions are given by Murzin and van Santen et al. [50,51]. Recent research by Cao et al. on the hydrogenation of LA using both Ru/Al_2O_3 and Ru/C catalysts also revealed the presence of typical volcano-type activity plots when the TOF was plotted as a function of the average Ru particle size [52]. A maximum TOF was found for catalyst with an average Ru particle diameter of about 1.5 nm for both supports.

Our dataset is too limited to draw definite conclusions regarding the optimal Ru nanoparticle size for the hydrogenation of LA, but seems to be between 1 and 3 nm for catalysts prepared with the two chloride precursors, $RuCl_3$, $Ru(NH_3)_6Cl_3$ and between 1 and 4 nm for $RuNO(NO_3)_3$, in line with the data from Cao et al. for Ru/Al_2O_3 and Ru/C catalysts.

Of interest is the observation that the highest TOF value in the range is observed for the catalyst prepared with the $RuNO(NO_3)_3$ precursor. One of the possible reasons for a better performance of the catalysts prepared with this precursor is the absence of chloride residues, which may be present when using the other two chlorine containing precursors. Analyses of the reduced catalysts by XPS shows the presence of only minor amounts of precursor-related elements. The content of Cl in Ru/TiO_2(Cl,N,10) catalyst is below 0.6 at.%, whereas it is below the detection limit for Ru/TiO_2(NO,N,10) and Ru/TiO_2(NH_3,N,10). As such, there is not a clear relation between the activity of the catalysts and the chlorine content of the samples. The nitrogen content in the three samples was also below the detection limit, indicating that differences in residual nitrogen content do not play a role.

Catalyst activity thus depends on Ru nanoparticle size; the observation that the activity versus Ru-nanoparticle size plots are also a function of the precursor used during synthesis, also suggests that other factors play a role as well, however. These can include the ratio of various charged and non-charged Ru species, or the presence of minor amounts of residues from the catalyst precursors.

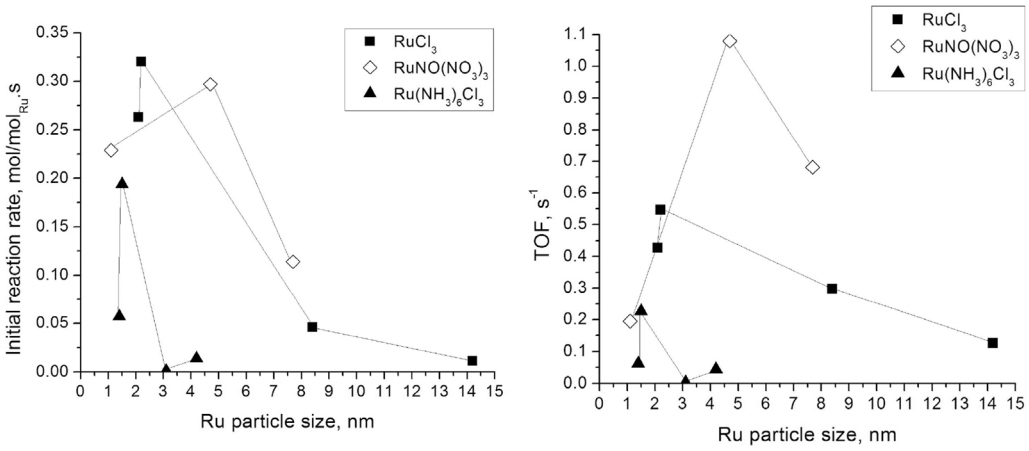

Fig. 7. Initial rate and TOF for LA hydrogenation in water versus the average Ru-nanoparticle for the Ru/TiO_2 catalysts prepared in this study according to TEM. Reaction conditions: see Table 2.

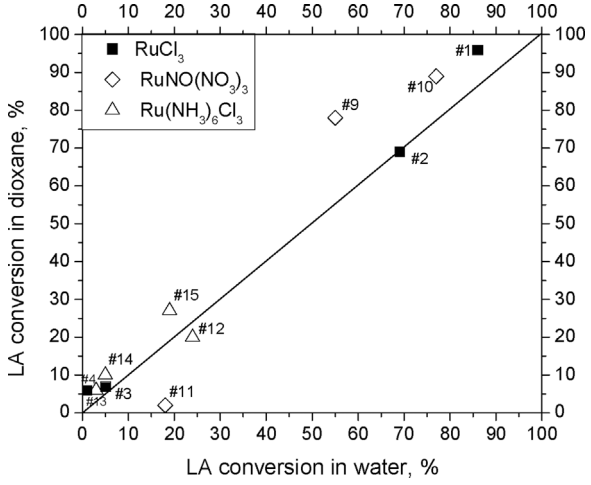

Fig. 8. Parity plot with the LA conversion after 4 h reaction time in water and dioxane.

3.6.2. Solvent effect

The hydrogenation reactions as reported in this study were carried out both in water and dioxane (see Table 2 for experimental details). Comparison of the LA conversion after 4 h reaction time for both water and dioxane in the form of a parity plot is provided in Fig. 8. A reasonable fit was obtained, showing that the performance in water and dioxane follow a similar trend. As such, the effect of Ru particle size distribution on catalytic activity as shown for water, seems to be valid for dioxane as well. In addition, it suggests that the molecular mechanism for the hydrogenation reactions in both solvents is similar.

4. Conclusions

We have shown that the performance of Ru/TiO_2 catalysts for the hydrogenation of LA in water and dioxane strongly depends on the preparation protocol (nature of the Ru-precursor, calcination and/or reduction step and the amount of hydrogen present in the sweep gas during reduction). Best results were obtained when using the $RuCl_3$ precursor (when considering initial rate on Ru intake) and the $RuNO(NO_3)_3$ precursor (when considering TOF) without an intermediate calcination step and 10% hydrogen in the reduction gas, whereas calcination and the use of a hydrogen rich sweep gas gave rise to lower catalytic activity. Catalyst characterization studies showed that the different preparation protocols lead to catalysts with differences in average Ru particle sizes. It was shown that catalyst activity (TOF and initial rates) in both water and dioxane is strongly correlated with the average Ru particle size, and an optimum activity was found for average Ru particle sizes of about 1–5 nm. This implies that LA hydrogenation in water is structure sensitive. The fact that catalysts with similar particle sizes though prepared with different precursors show different TOF values suggest that additional factors than particle size-dependent structure sensitivity must play a role. A possible factor is the difference in amounts of charged and neutral ruthenium species, which are expected to have different activity profiles. However, the influence of minor amounts of precursor residues such as Cl, as found for Ru/TiO_2 (Cl,N,10), cannot be ruled out.

Acknowledgements

This research was conducted in the framework of the Dutch CatchBio program. Financial support from the Smart Mix Program of the Netherlands Ministry of Economic Affairs and The Netherlands Ministry of Education, Culture and Science is gratefully acknowledged. The authors thank the members of the CatchBio User Committee for valuable suggestions and discussions. A. Goryachev J.P. Hofmann and E. J. M. Hensen from the Laboratory of Inorganic Materials Chemistry, Department of Chemical Engineering and Chemistry, Eindhoven University of Technology, The Netherlands are gratefully acknowledged for the XPS analyses.

Appendix A. Supplementary data

Supplementary data associated with this article can be found, in the online version, at http://dx.doi.org/10.1016/j.apcata.2017.09.032.

References

[1] D.W. Rackemann, W.O.S. Doherty, Biofuel. Bioprod. Biorefin. 5 (2011) 198–214.
[2] J.-P. Lange, Angew. Chem. Int. Ed. 54 (2015) 13186–13197.
[3] F. Rataboul, N. Essayem, Ind. Eng. Chem. Res. 50 (2011) 799–805.
[4] M.G. Al-Shaal, A. Dzierbinski, R. Palkovits, Green Chem. 16 (2014) 1358–1364.
[5] P.P. Upare, J.M. Lee, Y.K. Hwang, D.W. Hwang, J.H. Lee, S.B. Halligudi, ChemSusChem 4 (2011) 1749–1752.
[6] E.I. Gürbüz, D.M. Alonso, J.Q. Bond, J.A. Dumesic, ChemSusChem 4 (2011) 357–361.
[7] B. Chen, F. Li, Z. Huang, T. Lu, Y. Yuan, G. Yuan, ChemSusChem 7 (2014) 202–209.
[8] P. Neves, S. Lima, M. Pillinger, S.M. Rocha, J. Rocha, A.A. Valente, Catal. Today 218-219 (2013) 76–84.
[9] L. Manzer, Appl. Catal. A 272 (2004) 249–256.
[10] I.T. Horváth, H. Mehdi, V. Fábos, L. Boda, L.T. Mika, Green Chem. 10 (2008) 238–242.
[11] A. Strádi, M. Molnár, M. Óvári, G. Dibó, F.U. Richter, L.T. Mika, Green Chem. 15 (2013) 1857–1862.
[12] L. Qi, Y.F. Mui, S.W. Lo, M.Y. Lui, G.R. Akien, I.T. Horváth, ACS Catal. 4 (2014) 1470–1477.
[13] A.B. Kellicutt, R. Salary, O.A. Abdelrahman, J.Q. Bond, Catal. Sci. Technol. 4 (2014) 2267–2279.
[14] L.E. Manzer, US Patent No. US6617464 (2003).
[15] M. Chalid, A.A. Broekhuis, H.J. Heeres, J. Mol. Catal. A 341 (2011) 14–21.
[16] A.M. Raspolli Galletti, C. Antonetti, E. Riberchini, M.P. Colombini, N. Di Nasso, E. Bonari, Appl. Energy 102 (2013) 157–162.

[17] F. Liguori, C. Moreno-Marrodan, P. Barbaro, ACS Catal. 5 (2015) 1882–1894.
[18] S.G. Wettstein, D.M. Alonso, Y. Chong, J.A. Dumesic, Energy Environ. Sci. 5 (2012) 8199–8203.
[19] W. Luo, U. Deka, A.M. Beale, E.R.H. van Eck, P.C.A. Bruijnincx, B.M. Weckhuysen, J. Catal. 301 (2013) 175–186.
[20] W. Luo, M. Sankar, A.M. Beale, Q. He, C.J. Kiely, P.C.A. Bruijnincx, B.M. Weckhuysen, Nat. Commun. 6 (2015) 6540.
[21] D.M. Alonso, S.G. Wettstein, J.A. Dumesic, Green Chem. 15 (2013) 584–595.
[22] Z.P. Yan, L. Lin, S. Liu, Energy Fuels 23 (2009) 3853–3858.
[23] M. Chalid, Levulinic Acid as a Renewable Source for Novel Polymers, PhD Thesis, University of Groningen, The Netherlands, 2012.
[24] A.M. Raspolli Galletti, C. Antonetti, V. De Luise, M. Martinelli, Green Chem. 14 (2012) 688–694.
[25] M.G. Al-Shaal, W.R.H. Wright, R. Palkovits, Green Chem. 14 (2012) 1260–1263.
[26] D. Ding, J. Wang, J. Xi, X. Liu, G. Lu, Y. Wang, Green Chem. 16 (2014) 3846–3853.
[27] J.C. Serrano-Ruiz, D. Wang, J.A. Dumesic, Green Chem. 12 (2010) 574–577.
[28] J.-P. Lange, R. Price, P.M. Ayuob, J. Louis, L. Petrus, L. Clarke, H. Gosselink, Angew. Chem. 122 (2010) 4581–4585.
[29] J. Tan, J. Cui, T. Deng, X. Cui, G. Ding, Y. Zhu, Y. Li, ChemCatChem 7 (2015) 508–512.
[30] A.S. Piskun, J.M.G. Winkelman, Z. Tang, H.J. Heeres, H.J. Catalysts 6 (9) (2016) 131–151.
[31] Y. Kuwahara, W. Kaburagi, T. Fujitani, RSC Adv. 4 (2014) 45848–45855.
[32] A.M. Ruppert, J. Grams, M. Jędrzejczyk, J. Matras-Michalska, N. Keller, K. Ostojska, P. Sautet, ChemSusChem 8 (2015) 1538–1547.
[33] O.A. Abdelrahman, H.Y. Luo, A. Heyden, Y. Román-Leshkov, J.Q. Bond, J. Catal. 329 (2015) 10–21.
[34] V.V. Kumar, G. Naresh, M. Sudhakar, J. Tardio, S.K. Bhargava, A. Venugopal, Appl. Catal. A 505 (2015) 217–223.
[35] A.S. Piskun, J.E. de Haan, E. Wilbers, H.H. van de Bovenkamp, Z. Tang, H.J. Heeres, ACS Sustain. Chem. Eng. 4 (2016) 2939–2950.
[36] K. Hengst, M. Schubert, H.W.P. Carvalho, C. Lu, W. Kleist, J.-D. Grunwaldt, Appl. Catal. A 502 (2015) 18–26.
[37] W. Luo, P.C.A. Bruijnincx, B.M. Weckhuysen, J. Catal. 320 (2014) 33–41.
[38] A.S. Piskun, H.H. van de Bovenkamp, C.B. Rasrendra, J.G.M. Winkelman, H.J. Heeres, Appl. Catal. A 525 (2016) 1–10.
[39] J. Ftouni, A. Munoz-Murillo, A. Goryachev, J.P. Hofmann, E.J.M. Hensen, L. Lu, C.J. Kiely, P.S.A. Bruijnincx, B.M. Weckhuysen, ACS Catal. 6 (8) (2016) 5462–5472.
[40] H.S. Fogler, Elements of Chemical Reaction Engineering, fourth edition, (2006).
[41] C. Michel, P. Gallezot, ACS Catal. 5 (2015) 4130–4132.
[42] C. Michel, J. Zaffran, A.M. Ruppert, J. Matras-Michalska, M. Jędrzejczyk, J. Grams, P. Sautet, Chem. Commun. 50 (2014) 12450–12453.
[43] R. Luque, J.H. Clark, Cat. Comm. 11 (2010) 928–931.
[44] P. Panagiotopoulou, D.G. Vlachos, Appl. Catal. A 480 (2014) 17–24.
[45] P. Panagiotopoulou, N. Martin, D.G. Vlachos, J. Mol. Catal. A 392 (2014) 223–228.
[46] P. Reyes, M.E. König, G. Pecchi, I. Concha, M. López Granados, J.L.G. Fierro, Catal. Lett. 46 (1997) 71–75.
[47] Y. Zhang, X. Wang, Y. Zhu, T. Zhang, Appl. Catal. B 129 (2013) 382–393.
[48] C. Hernandez-Mejia, E.S. Gnanakumar, A. Olivos-Suarez, J. Gascon, H.F. Greer, W. Zhou, G. Rothenberg, N.R. Shiju, Catal. Sci. Technol. 6 (2016) 577–582.
[49] A. Primo, P. Concepción, A. Corma, Chem. Commun. 47 (2011) 3613–3615.
[50] D.Y. Murzin, J. Catal. 276 (2010) 85–91.
[51] R.A. van Santen, Acc. Chem. Res. 42 (2009) 57–66.
[52] S. Cao, J.R. Monnier, C.T. Williams, W. Diao, J.R. Regalbuto, J. Catal. 326 (2015) 69–81.